PHYSICAL REVIEW D **88,** 013017 (2013)

Explanation of the muon $g-2$ anomaly with vectorlike leptons and its implications for Higgs decays

Radovan Dermíšek* and Aditi Raval†

Physics Department, Indiana University, Bloomington, Indiana 47405, USA

(Received 31 May 2013; published 26 July 2013)

The deviation of the measured value of the muon anomalous magnetic moment from the standard model prediction can be completely explained by the mixing of the muon with extra vectorlike leptons, L and E, near the electroweak scale. This mixing simultaneously contributes to the muon mass. We show that the correlation between contributions to the muon mass and muon $g-2$ is controlled by the mass of the neutrino originating from the doublet L. Positive correlation, simultaneously explaining both measured values, requires this mass below 200 GeV. The decay rate of the Higgs boson to muon pairs is modified and, in the region of the parameter space that can explain the muon anomalous magnetic moment within one standard deviation, it ranges from 0.5 to 24 times the standard model prediction. In the same scenario, $h \to \gamma\gamma$ can be enhanced or lowered by $\sim 50\%$ from the standard model prediction. The explanation of the muon $g-2$ anomaly and predictions for $h \to \gamma\gamma$ are not correlated since these are controlled by independent parameters. This scenario can be embedded in a model with three complete vectorlike families featuring gauge coupling unification, sufficiently stable proton, and the Higgs quartic coupling remaining positive all the way to the grand unification scale.

DOI: 10.1103/PhysRevD.88.013017 PACS numbers: 13.40.Em, 12.60.−i, 14.60.Ef

I. INTRODUCTION

The measured value of the muon anomalous magnetic moment represents one of the largest discrepancies from predictions of the standard model (SM). There has been a variety of new physics models attempting to explain this deviation [1]. Most of the effort has been within the frameworks related to the explanation of the hierarchy between the electroweak (EW) scale and the grand unification (GUT) scale or the Planck scale.

However, we continue to see no signs of new physics related to solving the hierarchy problem at the LHC, and many well motivated possible explanations of the muon $g-2$ anomaly are now excluded. This motivates us to step back and see whether there are other simple ways to explain the anomaly that are testable at the LHC but not necessarily related to the naturalness problem of the electroweak symmetry breaking.

In this paper we show that the deviation of the measured value of the muon anomalous magnetic moment from the standard model prediction can be completely explained by the mixing of the muon with extra vectorlike leptons, L and E, near the electroweak scale. This mixing simultaneously contributes to the muon mass. We find that the correlation between contributions to the muon mass and muon $g-2$ is controlled by the mass of the neutrino originating from the doublet L, which is given by the vectorlike mass parameter M_L. Positive correlation, simultaneously explaining both measured values, requires this parameter to be small, $M_L \lesssim 200$ GeV. We further discuss implication of this scenario for Higgs decays, namely, $h \to \mu^+\mu^-$ and $h \to \gamma\gamma$, and provide a UV embedding of this scenario with many attractive features.

The possibility of explaining the muon $g-2$ anomaly by the mixing of the muon with extra heavy leptons was previously noticed in Refs. [2,3]. The mass enhancement originating from the loop involving a heavy lepton is compensated by small flavor violating couplings (which originate from the mixing, and thus they are suppressed by the mass of the heavy lepton). Therefore, the new physics contribution to the muon $g-2$, with new fermions at or below the TeV scale, can be of the same order as the contributions of the W and Z bosons in the standard model. A similar effect can be obtained with a Z' with flavor violating couplings of the muon to a heavier lepton; see, for example, Ref. [4].

Indeed, in several scenarios with new leptons near the EW scale explored recently in Ref. [3], it was found that the size of the muon $g-2$ anomaly is naturally of the same order as the contribution generated by heavy leptons, when their contribution to the muon mass is comparable to the physical muon mass. However, it was found that a positive contribution to the muon mass results in a negative contribution to the muon $g-2$ and vice versa. This was explored in the asymptotic limit of taking masses of extra leptons large while keeping the mixing with the muon constant (by increasing Yukawa couplings). We will show that this anticorrelation only happens in the asymptotic limit due to the dominance of the Higgs contribution. For smaller masses, it is the W contribution, controlled by M_L, that dominates. This reverses the sign of the correlation, and a simultaneous explanation of the muon mass and muon $g-2$ from the mixing can be achieved, and it is

*dermisek@indiana.edu
†adiraval@indiana.edu

fairly generic for small M_L.[1] In addition, an arbitrary correlation can be achieved in between the small M_L case, dominated by the W loop, and the asymptotic case, dominated by the Higgs loop.

The mixing of the muon with heavy leptons generically leads to a modification of the Higgs coupling to the muon [3,5]. Thus, the decay rate of the Higgs boson to muon pairs is modified, and in the region of the parameter space that can explain the muon $g-2$ within 1σ, it ranges from $\sim$0.5 to $\sim$24 times the standard model prediction. A part of the parameter space is already excluded by the ATLAS search for $h \to \mu^+\mu^-$, which with 20.7 fb^{-1} collected at 8 TeV sets the limit 9.8 times the SM prediction [6].

The scenario also allows for a sizable modification of $h \to \gamma\gamma$, since extra charged leptons can appear in loops mediating this process. This was recently extensively discussed in Refs. [7–10], motivated by the observed rate for $h \to \gamma\gamma$ at both the ATLAS and CMS experiments being significantly above the SM prediction at some point. However, with more data collected, the current ATLAS result is 1.65 ± 0.35 times the SM prediction [11], while the CMS experiment finds 0.78 ± 0.27 [12]. In the region of the parameter space that can explain the muon $g-2$ within 1σ, limiting the size of Yukawa couplings to 0.5, motivated by a simple UV embedding, the branching ratio for $h \to \gamma\gamma$ can be enhanced by $\sim$15% or lowered by $\sim$25%. Allowing Yukawa couplings of order 1, the $h \to \gamma\gamma$ rate can be modified by $\sim$50%. The explanation of the muon $g-2$ anomaly and predictions for $h \to \gamma\gamma$ are, however, not correlated since these are controlled by independent parameters.

Models with flavor violating couplings are typically highly constrained by limits on a variety of flavor changing precesses. However, these constraints involve products of flavor violating couplings of two different light leptons, while for the explanation of the muon $g-2$ anomaly, only the couplings of the muon to heavy leptons are necessary. We can therefore take the existing limits on flavor violating processes as constraints on other couplings in the model that are not necessary for the explanation of the muon $g-2$ anomaly.

While the extra vectorlike leptons, L and E, that mix with the muon are sufficient for the explanation of the muon $g-2$ anomaly, this does not have to be the full story. The model can be combined with other scenarios involving vectorlike fermions. For example, it is possible to embed it into a recently discussed scenario with extra three or more complete vectorlike families [13,14] featuring gauge coupling unification, a sufficiently stable proton, and the Higgs quartic coupling remaining positive all the way to the GUT scale. In this scenario, predicted values of gauge couplings at the electroweak scale are highly insensitive to GUT scale parameters and masses of vectorlike fermions. They can be understood from IR fixed point predictions and threshold effects from integrating out vectorlike families. Furthermore, a model with extra Z' and vectorlike quarks was recently discussed as a possible explanation of the anomalies in Z-pole observables: the forward-backward asymmetry of the b quark and the lepton asymmetry obtained from the measurement of left-right asymmetry for hadronic final states [15,16]. These two scenarios could also be combined, and a simultaneous explanation of anomalies in Z-pole observables and the muon $g-2$ could be obtained.

This paper is organized as follows. In Sec. II, we define the model and find expressions for couplings of Z, W, and h to the SM and extra leptons. In Sec. III, we calculate contributions of extra leptons to the muon anomalous magnetic moment, qualitatively discuss expected results, provide results from numerical scans over the parameters space, and discuss the predictions from the regions that explain the muon $g-2$ for Higgs decays, namely, $h \to \mu^+\mu^-$ and $h \to \gamma\gamma$. We also discuss constraints from precision EW observables and current constraints from the LHC and encourage further searches for extra leptons in a variety of final states at the LHC. In Sec. IV, we discuss a possible UV embedding of this model in the extension of the SM with three complete vectorlike families. We provide some concluding remarks in Sec. V.

II. MODEL

Quantum numbers of SM particles and an extra vectorlike family (VF) are summarized in Table I. The notation is straightforward; we use lower case letters for standard model particles and upper case letters for particles from extra VF, e.g., E_R has the same quantum numbers as e_R, and its vectorlike partner is E_L. For the discussion of the muon $g-2$, only $L_{L,R}$ and $E_{L,R}$ are relevant. Extra quarks obviously do not contribute, and we will not assume that the standard model singlets $N_{L,R}$ are near the EW scale.

The most general renormalizable Lagrangian for charged leptons is given by

$$\mathcal{L} \supset -\bar{l}_{Li} y_{ij} e_{Rj} H - \bar{l}_{Li} \lambda^E_i E_R H - \bar{L}_L \lambda^L_j e_{Rj} H - \lambda \bar{L}_L E_R H - \bar{\lambda} H^\dagger \bar{E}_L L_R - M_L \bar{L}_L L_R - M_E \bar{E}_L E_R + \text{H.c.}, \quad (1)$$

where the first five terms represent the usual standard model Yukawa couplings (the sum over flavor indices is assumed), Yukawa couplings between SM leptons and leptons from the VF, and between leptons from the VF. The last two terms are mass terms for vectorlike pairs of leptons. We label the components of doublets as follows:

[1]This possibility was missed in the original version of Ref. [3] as a result of a mistake in the calculation of the W contribution. It was pointed out by one of the authors of this paper, A. R. In the corrected version of Ref. [3], some points with a positive correlation between contributions to the muon $g-2$ and muon mass appeared, but the focus of the paper remained on the asymptotic case.

TABLE I. Quantum numbers of standard model and extra vectorlike particles. The electric charge is given by $Q = T_3 + Y$, where T_3 is the weak isospin, which is $+1/2$ for the first component of a doublet and $-1/2$ for the second component.

	q_L	u_R	d_R	l_L	ν_R	e_R	H	$Q_{L,R}$	$U_{L,R}$	$D_{L,R}$	$L_{L,R}$	$N_{L,R}$	$E_{L,R}$
$SU(3)_C$	**3**	**3**	**3**	**1**	**1**	**1**	**1**	**3**	**3**	**3**	**1**	**1**	**1**
$SU(2)_L$	**2**	**1**	**1**	**2**	**1**	**1**	**2**	**2**	**1**	**1**	**2**	**1**	**1**
$U(1)_Y$	$\frac{1}{6}$	$\frac{2}{3}$	$-\frac{1}{3}$	$-\frac{1}{2}$	0	-1	$\frac{1}{2}$	$\frac{1}{6}$	$\frac{2}{3}$	$-\frac{1}{3}$	$-\frac{1}{2}$	0	-1

$$l_{Li}=\begin{pmatrix}\nu_i\\ e_{Li}\end{pmatrix},\quad L_{L,R}=\begin{pmatrix}L^0_{L,R}\\ L^-_{L,R}\end{pmatrix},\quad H=\begin{pmatrix}0\\ v+\frac{h}{\sqrt{2}}\end{pmatrix}, \quad (2)$$

where $v = 174$ GeV is the vacuum expectation value of the Higgs field.

After spontaneous symmetry breaking, the 5×5 mass matrix for charged leptons is given by

$$(\bar{e}_{Li},\bar{L}^-_L,\bar{E}_L)M_e\begin{pmatrix}e_{Rj}\\ L^-_R\\ E_R\end{pmatrix} =(\bar{e}_{Li},\bar{L}^-_L,\bar{E}_L)\begin{pmatrix}y_{ij}v & 0 & \lambda^E_i v\\ \lambda^L_j v & M_L & \lambda v\\ 0 & \bar{\lambda}v & M_E\end{pmatrix}\begin{pmatrix}e_{Rj}\\ L^-_R\\ E_R\end{pmatrix}, \quad (3)$$

and it is convenient to define 5-component vectors: $e_{La}\equiv(e_{Li}, L^-_L, E_L)^T$ (and similarly for e_{Ra} with $L\to R$), which combine the left- (right-)handed fields of the SM with those from the extra vectorlike pairs. We use indices from the beginning of the alphabet for combined vectors and indices starting with i for only the standard model leptons. This mass matrix can be diagonalized by a biunitary transformation, $U^\dagger_L M_e U_R$, which defines the mass eigenstate basis. We label the mass eigenstates by e_a, and for the lightest three eigenstates we will also use their names: e, μ, and τ.

Before diagonalizing the full mass matrix, it is instructive to change the basis by a unitary transformation, $e_{Li}\to(V_L e_L)_i$, $e_{Rj}\to(V_R e_R)_j$, which diagonalizes the standard model Yukawa couplings y_{ij}. The mass matrix becomes

$$\begin{pmatrix}(V^\dagger_L y V_R)_{ij}v & 0 & (V^\dagger_L)_{ik}\lambda^E_k v\\ \lambda^L_l (V_R)_{lj}v & M_L & \lambda v\\ 0 & \bar{\lambda}v & M_E\end{pmatrix}. \quad (4)$$

Since we are interested in modifying couplings of the muon, we assume that only $(V^\dagger_L)_{2k}\lambda^E_k$ and $\lambda^L_l (V_R)_{l2}$ are nonzero. This corresponds to the situation when $\lambda^E_k\propto(V_L)_{k2}$ and $\lambda^L_l\propto(V^\dagger_R)_{2l}$, or in the basis where standard model Yukawa couplings are diagonal, it corresponds to $\lambda^{L,E}_1=\lambda^{L,E}_3=0$, and $\lambda^{L,E}_2\equiv\lambda^{L,E}$ is nonzero. This is the minimal scenario that does not modify standard model couplings of the electron and tau.

In this minimal scenario, masses of the electron and tau fully originate from their Yukawa couplings to the Higgs boson since they do not mix with heavy leptons. Therefore, we can look at the 3×3 mass matrix for the muon and the extra heavy leptons separately:

$$U^\dagger_L\begin{pmatrix}y_\mu v & 0 & \lambda^E v\\ \lambda^L v & M_L & \lambda v\\ 0 & \bar{\lambda}v & M_E\end{pmatrix}\quad U_R=\begin{pmatrix}m_\mu & 0 & 0\\ 0 & m_{e_4} & 0\\ 0 & 0 & m_{e_5}\end{pmatrix}, \quad (5)$$

where we use the same names for diagonalization matrices $U_{L,R}$ as for the matrices that diagonalize the general 5×5 matrix. We label their components by 2, 4, and 5 so that results are applicable to the general scenario. Similarly we label the heavy mass eigenstates by e_4 and e_5.

In the limit

$$\lambda_E v,\ \lambda_L v,\ \bar{\lambda}v,\ \lambda v \ll M_E, M_L, \quad (6)$$

approximate analytic formulas for diagonalization matrices can be obtained, which are useful for deriving approximate formulas for couplings of Z, W, and h. In this limit, the two heavy charged leptons have masses close to M_L and M_E. In the basis (m_μ, $m_{e_4}\simeq M_L$, $m_{e_5}\simeq M_E$), the diagonalization matrices are given by

$$U_L=\begin{pmatrix}1-v^2\frac{\lambda_E^2}{2M_E^2} & -v^2\left(\frac{\lambda_E}{M_L}\frac{\bar{\lambda}M_E+\lambda M_L}{M_E^2-M_L^2}-\frac{y_\mu\lambda_L}{M_L^2}\right) & v\frac{\lambda_E}{M_E}\\ v^2\frac{\bar{\lambda}\lambda_E M_L-y_\mu\lambda_L M_E}{M_L^2 M_E} & 1-v^2\frac{(\lambda M_E+\bar{\lambda}M_L)^2}{2(M_E^2-M_L^2)^2} & v\frac{\bar{\lambda}M_L+\lambda M_E}{M_E^2-M_L^2}\\ -v\frac{\lambda_E}{M_E} & -v\frac{\bar{\lambda}M_L+\lambda M_E}{M_E^2-M_L^2} & 1-v^2\frac{\lambda_E^2}{2M_E^2}-v^2\frac{(\lambda M_E+\bar{\lambda}M_L)^2}{2(M_E^2-M_L^2)^2}\end{pmatrix} \quad (7)$$

and

$$U_R = \begin{pmatrix} 1 - v^2 \frac{\lambda_L^2}{2M_L^2} & v \frac{\lambda_L}{M_L} & v^2 \left(\frac{\lambda_L}{M_E} \frac{\bar{\lambda} M_L + \lambda M_E}{M_E^2 - M_L^2} + \frac{y_\mu \lambda_E}{M_E^2} \right) \\ -v \frac{\lambda_L}{M_L} & 1 - v^2 \frac{\lambda_L^2}{2M_L^2} - v^2 \frac{(\bar{\lambda} M_E + \lambda M_L)^2}{2(M_E^2 - M_L^2)^2} & v \frac{\bar{\lambda} M_E + \lambda M_L}{M_E^2 - M_L^2} \\ v^2 \frac{\lambda_L \bar{\lambda} M_E - y_\mu \lambda_E M_L}{M_L M_E^2} & -v \frac{\bar{\lambda} M_E + \lambda M_L}{M_E^2 - M_L^2} & 1 - v^2 \frac{(\bar{\lambda} M_E + \lambda M_L)^2}{2(M_E^2 - M_L^2)^2} \end{pmatrix}. \tag{8}$$

A. Couplings of the Z boson and photon

Couplings of the electron and τ to the Z boson are not modified from their SM values. Couplings of other charged leptons to the Z boson are modified because the extra E_L is an SU(2) singlet, but it mixes with SU(2) doublets, and L_R^- originates from an SU(2) doublet, but it mixes with SU(2) singlets. The couplings follow from the kinetic terms:

$$\begin{aligned} \mathcal{L}_{\rm kin} &\supset \bar{e}_{La} i \not{\partial}_a e_{La} + \bar{e}_{Ra} i \not{\partial}_a e_{Ra} \\ &= \bar{\hat{e}}_{La} (U_L^\dagger)_{ac} i \not{\partial}_c (U_L)_{cb} \hat{e}_{Lb} + \bar{\hat{e}}_{Ra} (U_R^\dagger)_{ac} i \not{\partial}_c (U_R)_{cb} \hat{e}_{Rb}, \end{aligned} \tag{9}$$

where the vectors of mass eigenstates are $\hat{e}_{La} \equiv (\hat{\mu}_L, \hat{e}_{L4}, \hat{e}_{L5})^T$ and similarly for $\hat{e}_R$. The covariant derivative is given by

$$D_{\mu a} = \partial_\mu - i \frac{g}{\cos\theta_W} (T_a^3 - \sin^2\theta_W Q_a) Z_\mu - i e Q_a A_\mu, \tag{10}$$

where the weak isospin T^3 and the electric charge Q for a given field can be obtained from Table I. Defining couplings of the Z boson to fermions f_a and f_b by the Lagrangian of the form

$$\mathcal{L} \supset (\bar{f}_{La} \gamma^\mu g_L^{Z f_a f_b} f_{Lb} + \bar{f}_{Ra} \gamma^\mu g_R^{Z f_a f_b} f_{Rb}) Z_\mu, \tag{11}$$

we find the couplings of left- and right-handed fields:

$$g_L^{Z e_a e_b} = \frac{g}{\cos\theta_W} \sum_{c=2,4,5} (T_{Lc}^3 - \sin^2\theta_W Q_c) (U_L^\dagger)_{ac} (U_L)_{cb}, \tag{12}$$

$$g_R^{Z e_a e_b} = \frac{g}{\cos\theta_W} \sum_{c=2,4,5} (T_{Rc}^3 - \sin^2\theta_W Q_c) (U_R^\dagger)_{ac} (U_R)_{cb}, \tag{13}$$

where $Q_c = -1$ is the same for all states; $T_{Lc}^3 = -1/2$ for $c = 2, 4$, and 0 for $c = 5$; and $T_{Rc}^3 = 0$ for $c = 2, 5$, and $-1/2$ for $c = 4$.

Since $Q_c = -1$ for all the fields, couplings of the photon are not modified from their SM values by field rotations. However, due to different weak isospins of fields that mix, the couplings of the Z boson given in Eqs. (12) and (13) are modified. Corrections to the usual SM value of the left-handed charged lepton coupling,

$$(g_L^{Z e_a e_b})_{\rm SM} = \frac{g}{\cos\theta_W} \left(-\frac{1}{2} + \sin^2\theta_W \right) \delta^{ab}, \tag{14}$$

can be written as

$$\delta g_L^{Z e_a e_b} = \frac{g}{2\cos\theta_W} (U_L^\dagger)_{a5} (U_L)_{5b}. \tag{15}$$

Similarly, corrections to the usual SM value of the right-handed charged lepton coupling,

$$(g_R^{Z e_a e_b})_{\rm SM} = \frac{g}{\cos\theta_W} \sin^2\theta_W \delta^{ab}, \tag{16}$$

can be written as

$$\delta g_R^{Z e_a e_b} = -\frac{g}{2\cos\theta_W} (U_R^\dagger)_{a4} (U_R)_{4b}. \tag{17}$$

B. Couplings of the W boson

The couplings of the electron and τ to the W boson are not modified from their SM values. Couplings of other charged leptons follow from the kinetic terms:

$$\mathcal{L}_{\rm kin} \supset \frac{g}{\sqrt{2}} (\bar{\nu}_\mu \gamma^\mu \mu_L + \bar{L}_L^0 \gamma^\mu L_L^- + \bar{L}_R^0 \gamma^\mu L_R^-) W_\mu^+ + \text{H.c.} \tag{18}$$

$$\begin{aligned} &= \frac{g}{\sqrt{2}} (\bar{\nu}_\mu \gamma^\mu (U_L)_{2b} \hat{e}_{Lb} + \bar{L}_L^0 \gamma^\mu (U_L)_{4b} \hat{e}_{Lb} \\ &\quad + \bar{L}_R^0 \gamma^\mu (U_R)_{4b} \hat{e}_{Rb}) W_\mu^+ + \text{H.c.} \end{aligned} \tag{19}$$

Defining couplings of the W boson to neutrinos ν_a and charged leptons $\hat{e}_b$ by the Lagrangian of the form

$$\mathcal{L} \supset (\bar{\nu}_{La} \gamma^\mu g_L^{W \nu_a e_b} \hat{e}_{Lb} + \bar{\nu}_{Ra} \gamma^\mu g_R^{W \nu_a e_b} \hat{e}_{Rb}) W_\mu^+ + \text{H.c.}, \tag{20}$$

we find couplings of left- and right-handed fields:

$$g_L^{W \nu_\mu e_b} = \frac{g}{\sqrt{2}} (U_L)_{2b}, \qquad g_L^{W \nu_4 e_b} = \frac{g}{\sqrt{2}} (U_L)_{4b}, \tag{21}$$

$$g_R^{W \nu_4 e_b} = \frac{g}{\sqrt{2}} (U_R)_{4b}. \tag{22}$$

C. Couplings of the Higgs boson

In the minimal scenario that we are focusing on, couplings of the electron and tau to the Higgs boson are given by the SM relations, $\lambda_{e,\tau} = m_{e,\tau}/v$. This usual relation between the mass of a particle and its coupling to the Higgs boson does not apply to other charged leptons as a

consequence of explicit mass terms for vectorlike fermions, M_E and M_L. The couplings of the Higgs boson for other charged leptons follow from the Yukawa terms:

$$\mathcal{L}_Y \supset -\frac{1}{\sqrt{2}}\bar{e}_{La}Y_{ab}e_{Rb}h + \text{H.c.} = -\frac{1}{\sqrt{2}}\bar{\hat{e}}_{La}(U_L^\dagger)_{ac}Y_{cd}(U_R)_{db}\hat{e}_{Rb}h + \text{H.c.}, \quad (23)$$

where

$$Y = \begin{pmatrix} y_\mu & 0 & \lambda^E \\ \lambda^L & 0 & \lambda \\ 0 & \bar{\lambda} & 0 \end{pmatrix}. \quad (24)$$

Since the Y matrix is not proportional to the mass matrix given in Eq. (5), the Higgs couplings are in general flavor violating. Defining couplings of the Higgs boson to mass eigenstates fermions f_a and f_b by the Lagrangian of the form

$$\mathcal{L} \supset -\frac{1}{\sqrt{2}}\bar{f}_{La}\lambda_{f_af_b}f_{Rb}h + \text{H.c.}, \quad (25)$$

we find

$$\lambda_{e_ae_b} = \sum_{c,d=2,4,5}(U_L^\dagger)_{ac}Y_{cd}(U_R)_{db}. \quad (26)$$

Noticing that $Yv = M_e - \text{diag}(0, M_L, M_E)$, the Higgs boson couplings to mass eigenstates can be alternatively written as

$$\lambda_{e_ae_b}v = \begin{pmatrix} m_\mu & 0 & 0 \\ 0 & m_{e_4} & 0 \\ 0 & 0 & m_{e_5} \end{pmatrix} - U_L^\dagger \begin{pmatrix} 0 & 0 & 0 \\ 0 & M_L & 0 \\ 0 & 0 & M_E \end{pmatrix} U_R, \quad (27)$$

where the first term comes from the usual SM relation between fermion masses and their couplings to the Higgs boson, and the second term represents contributions from the $M_{L,E}$ terms.

In the limit (6), the approximate analytic formulas for all the couplings of Z, W, and h can be easily obtained from diagonalization matrices (7) and (8).

III. MUON ANOMALOUS MAGNETIC MOMENT

The discrepancy between the measured value of the muon anomalous magnetic moment [17] and the SM prediction,

$$\Delta a_\mu^{\text{exp}} = a_\mu^{\text{exp}} - a_\mu^{\text{SM}} = 2.7 \pm 0.80 \times 10^{-9}, \quad (28)$$

which we will use in our analysis, is the average of evaluations of this discrepancy reported by several groups: $2.49 \pm 0.87 \times 10^{-9}$ [18], $2.61 \pm 0.80 \times 10^{-9}$ [19], and $2.87 \pm 0.80 \times 10^{-9}$ [20]. On average, the discrepancy is at the level of 3.4 standard deviations.

The contributions to the muon magnetic moment from extra fermions originate from the loop diagrams with the Higgs, Z, and W bosons shown in Fig. 1. Our calculation of these contributions, presented below, agrees with the results in Refs. [21,22] and also in the revised version of Ref. [3]. For references to the original calculation of the Z, W, and h contributions in the SM, see Ref. [1].

The contribution from the Higgs diagram is given by

$$\delta a_\mu^h = -\frac{m_\mu}{32\pi^2 M_h^2}\sum_{b=4,5}[(|\lambda_{\mu e_b}|^2 + |\lambda_{e_b\mu}|^2)m_\mu F_h(x_{hb}) + \text{Re}(\lambda_{\mu e_b}\lambda_{e_b\mu})m_{e_b}G_h(x_{hb})], \quad (29)$$

where $x_{hb} \equiv (m_{e_b}/M_h)^2$, the couplings are given in Eq. (26) with index $\mu \equiv e_2$, and the loop functions are as follows:

$$F_h(x) = -\frac{x^3 - 6x^2 + 3x + 6x\ln(x) + 2}{6(1-x)^4}, \quad (30)$$

$$G_h(x) = \frac{x^2 - 4x + 2\ln(x) + 3}{(1-x)^3}. \quad (31)$$

The contribution from the Z diagram is given by

$$\delta a_\mu^Z = -\frac{m_\mu}{8\pi^2 M_Z^2}\sum_{b=4,5}[(|g_L^{Z\mu e_b}|^2 + |g_R^{Z\mu e_b}|^2)m_\mu F_Z(x_{Zb}) + \text{Re}(g_L^{Z\mu e_b}g_R^{Z\mu e_b *})m_{e_b}G_Z(x_{Zb})], \quad (32)$$

where $x_{Zb} = (m_{e_b}/M_Z)^2$, the couplings are given in Eqs. (12) and (13) with index $\mu \equiv e_2$, and the loop functions are as follows:

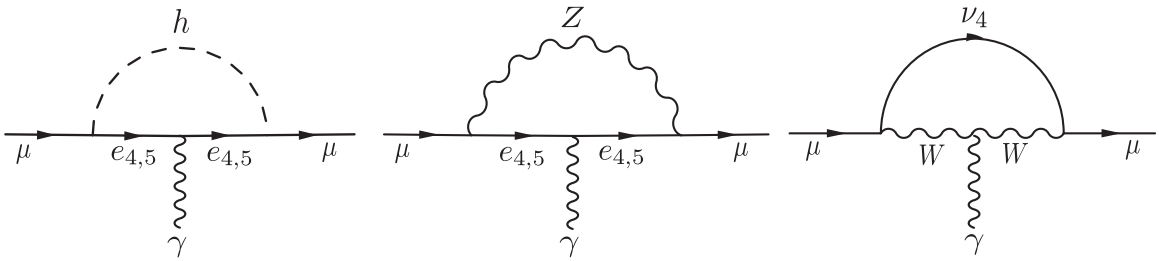

FIG. 1. Feynman diagrams contributing to the muon magnetic moment that involve loops of extra fermions and the Higgs, Z and W bosons.

$$F_Z(x) = \frac{5x^4 - 14x^3 + 39x^2 - 38x - 18x^2\ln(x) + 8}{12(1-x)^4}, \tag{33}$$

$$G_Z(x) = \frac{x^3 + 3x - 6x\ln(x) - 4}{2(1-x)^3}. \tag{34}$$

Finally, the contribution from the W diagram is given by

$$\delta a_\mu^W = -\frac{m_\mu}{16\pi^2 M_W^2}[(|g_L^{W\nu_4\mu}|^2 + |g_R^{W\nu_4\mu}|^2)m_\mu F_W(x_W) + \mathrm{Re}(g_L^{W\nu_4\mu} g_R^{W\nu_4\mu *})M_L G_W(x_W)], \tag{35}$$

where $x_W = (M_L/M_W)^2$ since the mass of ν_4 is given by M_L. The couplings are given in Eqs. (21) and (22) with index $\mu \equiv e_2$, and the loop functions are as follows:

$$F_W(x) = -\frac{4x^4 - 49x^3 + 78x^2 - 43x + 18x^3\ln(x) + 10}{6(1-x)^4}, \tag{36}$$

$$G_W(x) = -\frac{x^3 - 12x^2 + 15x + 6x^2\ln(x) - 4}{(1-x)^3}. \tag{37}$$

A. Qualitative analysis

An interesting insight can be obtained by integrating out vectorlike leptons [3]. In the limit (6), the muon mass, after EW symmetry breaking, receives contributions from two terms:

$$\mathcal{L}_{\mathrm{eff}} \supset -\bar{\mu}_L\left(y_\mu + \frac{\lambda^L\bar{\lambda}\lambda^E}{M_L M_E}HH^\dagger\right)\mu_R H + \mathrm{H.c.} \rightarrow -(m_\mu^H + m_\mu^{LE})\bar{\mu}_L\mu_R + \mathrm{H.c.}, \tag{38}$$

where m_μ^H originates from the direct Yukawa coupling of the muon flavor eigenstate and m_μ^{LE} comes from the mixing with vectorlike leptons. Due to the same chiral structure, the m_μ^{LE} term also contributes to the muon magnetic moment. This contribution can be written as

$$\Delta a_\mu \simeq c\frac{m_\mu m_\mu^{LE}}{(4\pi v)^2} \simeq 0.85c\frac{m_\mu^{LE}}{m_\mu}\Delta a_\mu^{\mathrm{exp}}. \tag{39}$$

In the limit $M_E \simeq M_L \gg M_Z$, it was found that $c = -1$ [3]. This means that the contributions to the muon mass and muon $g-2$ are anticorrelated. Nevertheless, ignoring the wrong sign, the size of the contribution to the muon $g-2$ is what is needed to explain the measured value when the muon mass originates mostly from the mixing with vectorlike leptons.

However, this conclusion holds only in the asymptotic region $M_E \simeq M_L \gg M_Z$. We can obtain a simple approximate formula for Δa_μ even in the region of small M_E and M_L. It turns out, that the formula (39) is still valid with c being a function of masses of extra fermions, which can be written as:

$$c = c_W(x_W) + c_Z(x_Z) + c_h(x_h) \simeq G_W(x_W) - 2. \tag{40}$$

The second part follows from $c_W(x_W) \simeq G_W(x_W)$ and the sum of the $c_Z(x_Z)$ and $c_h(x_h)$ being approximately -2 in a large range of masses, as a result of $G_Z(x)$ and $xG_h(x)$ changing slowly with x.

The Higgs contribution can be approximately written as $c_h(x_h) \simeq 3/2x_h G_h(x_h)$, where x_h is associated with the lighter of the two leptons.[2] It varies from -1 to $-3/2$ for x_h between 1 and ∞. Asymptotically, or if at least one of the masses of extra charged leptons is somewhat larger than M_Z, the Z contribution is given by $c_Z(x_Z) \simeq G_Z(x_Z)$, where the x_Z is associated with the heavier of the two leptons. Numerically, $c_Z(x_Z) \simeq -1/2$, which is the asymptotic value of $G_Z(x_Z)$. For both masses close to M_Z, we find $c_Z(x_Z) \simeq G_Z(x_Z) + x_Z G'(x_Z)$, which for $x_Z = 1$ equals $-3/4$. Therefore, the Z contribution varies from $-3/4$ to $-1/2$ for x_Z between 1 and ∞. Thus, the Z and Higgs contributions add up to ~ -2 for a large range of masses of vectorlike leptons.

The W contribution, $c_W(x_W) \simeq G_W(x_W)$, strongly depends on the mass of the heavy neutrino, which in our model is given by M_L. While its asymptotic value is $+1$ leading to total $c \simeq -1$, for $M_L \simeq M_W$ it is $+3$ leading to total $c \simeq +1$. Therefore, the correlation between contributions to the muon mass and muon $g-2$ is mostly controlled by M_L, and we have two solutions: the asymptotic one, $M_L \gg M_Z$, in which case the measured value of the muon $g-2$ is obtained for $m_\mu^{LE}/m_\mu \simeq -1$, and the second one with a light extra neutrino, $M_L \simeq M_W$, in which case the measured value of the muon $g-2$ is obtain for $m_\mu^{LE}/m_\mu \simeq +1$. In the first case, about twice as large a contribution from the direct Yukawa coupling of the muon is required to generate the correct muon mass, while in the second case, the muon mass can fully originate from the mixing with heavy leptons. Any other correlation between $+1$ and -1 can be obtained by increasing the M_L from the EW scale to the $\sim$1 TeV scale.

This is illustrated in Fig. 2 in which we show separate contributions to the muon $g-2$ and the c coefficient from Z, W, and h as functions of M_L. In both plots, we fix $M_E = 250$ GeV, $\bar{\lambda} = 0.5$, $\lambda = 0$, and λ_L and λ_E are set to their approximate maximum values allowed by precision EW data (discussed later), which fixes m_μ^{LE}. The almost identical shape of lines in both plots in Fig. 2 further supports the fact that Eq. (39) with c given in Eq. (40) is indeed a good approximation. Chosen signs of couplings in the plots correspond to generating a positive contribution to the muon mass from m_μ^{LE}. If the product $\lambda^L\bar{\lambda}\lambda^E$ is negative, leading to a negative contribution to the muon mass from

[2]In the derivation of this formula, we used the fact that $x_h G_h(x_h)$ varies very little with x_h. A better approximation is $c_h(x_h) \simeq x_{h4}G_h(x_{h4}) + 1/2x_{h5}G_h(x_{h5})$ when the masses of the two charged leptons are different, and $c_h(x_h) \simeq x_h G_h(x_h) - 1/2x_h^2 G'(x_h)$ when the masses are similar.

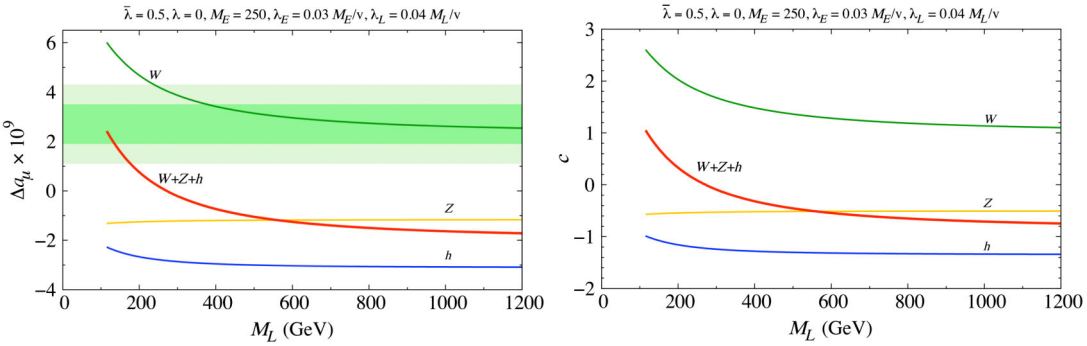

FIG. 2 (color online). Left: contributions to the muon $g-2$ from Z, W, and h loops with heavy leptons shown in Fig. 1 as functions of M_L. The sum of all contributions is also plotted. Dark and light shaded bands correspond to 1σ and 2σ regions of Δa_μ specified in Eq. (28). Right: separate and total contributions to the c coefficient defined by assuming the equality in Eq. (39) that shows the correlation between contributions of heavy leptons to the muon $g-2$ and the muon mass. In both plots, we fix $M_E = 250$ GeV, $\bar{\lambda} = 0.5$, $\lambda = 0$, and λ^L and λ^E are set to their approximate maximum allowed values given in Eq. (41). The signs of couplings are chosen so that m_μ^{LE} is positive. For the opposite sign of m_μ^{LE}, the signs on the y axis in the left plot should be flipped.

m_μ^{LE}, the $g-2$ plot would look identical with the signs on the y axis flipped.

The contributions to the c coefficient in Fig. 2, for a given choice of parameters, are representative for a large range of M_L and M_E. The plots would be almost identical for any larger value of M_E and would only slightly change in the small M_L region for M_E as small as 100 GeV. All the Yukawa couplings only rescale the contributions to the muon $g-2$; different choices do not change the results qualitatively as far as the condition (6) is satisfied.

B. Constraints

In the numerical scans over the parameter space that follow, we impose constraints from precision EW data related to the muon that include the Z pole observables (Z partial width, forward-backward asymmetry, left-right asymmetry), the W partial width, and the muon lifetime [23]. In the limit of small couplings (6), these constraints approximately translate into 95% C.L. bounds on $\lambda^{E,L}$ couplings:

$$\frac{\lambda^E v}{M_E} \lesssim 0.03, \qquad \frac{\lambda^L v}{M_L} \lesssim 0.04. \tag{41}$$

These quantities squared represent modifications of the SM couplings of the Z and W to the muon, which can be obtained from Eqs. (15), (17), and (21) and the diagonalization matrices (7) and (8). We further impose constraints from oblique corrections, namely, from S and T parameters [23]. Finally, we impose the large electron positron collider limits on masses of charged leptons, which are required to be larger than 105 GeV.

C. Scan over the parameter space: Muon $g-2$ and Higgs decays

The previous qualitative discussion of expected results is fully supported by numerical scans. In Fig. 3 on the left, we plot the contribution to the muon $g-2$ vs the contribution to the muon mass from the mixing with heavy leptons for randomly generated points with $M_L \in [100, 1000]$ GeV, $M_E \in [100, 1000]$ GeV, $\bar{\lambda} < 0.5$, and $\lambda_{L,E}$ in allowed ranges from precision EW data. For simplicity, λ is set to 0 in these plots because it should not have a significant effect on our results. In all the plots in this section the m_μ^{LE} is defined more precisely as the mass that the muon would have if the direct Yukawa coupling was zero. Different colors (shades) correspond to different regions of M_L. This shows that it is indeed M_L that controls the correlation between the contribution to the muon $g-2$ and muon mass.

There are two solutions: the asymptotic solution for large M_L, in which the measured muon $g-2$ can be obtained for $m_\mu^{LE}/m_\mu \simeq -1$ and so the physical muon mass is a result of a cancellation between the direct Yukawa coupling and the contribution from the mixing, and the light neutrino solution for $M_L \simeq 100$ GeV, in which case the muon mass can fully originate from the mixing, $m_\mu^{LE}/m_\mu \simeq +1$.[3]

On the right in Fig. 3, we plot the same points in the $\Delta a_\mu - R_{\mu\mu}$ plane, where

$$R_{\mu\mu} \equiv \frac{\Gamma(h \to \mu^+\mu^-)}{\Gamma(h \to \mu^+\mu^-)_{\rm SM}}. \tag{42}$$

This plot can be easily understood from Eq. (38). The enhancement of $\Gamma(h \to \mu^+\mu^-)$ by a factor of 9 compared to the SM in the small M_L case that can explain the muon $g-2$ anomaly, for which $m_\mu^{LE}/m_\mu \simeq +1$, originates from three possible ways one Higgs coupling and 2 vacuum

[3]In the corrected version of Ref. [3], there are solutions explaining the muon $g-2$ with significantly smaller m_μ^{LE} compared to our results. For these points, however, the new physics contribution to the muon mass was not calculated correctly, and there are indeed no such solutions [24].

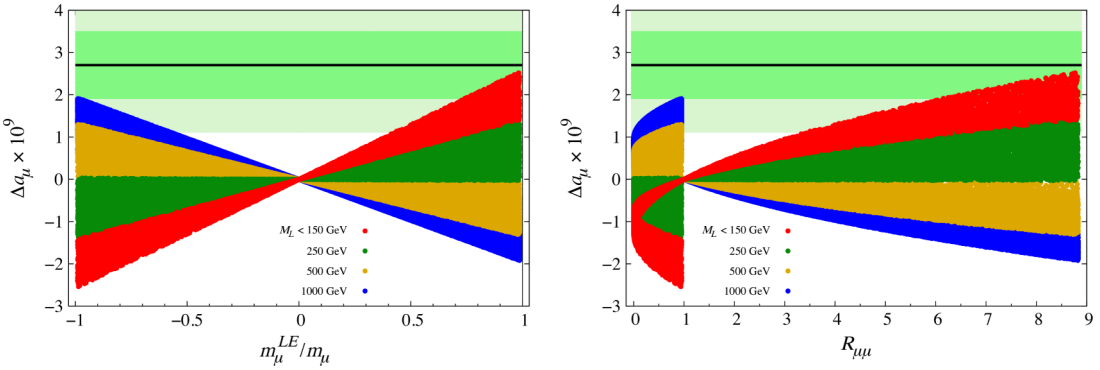

FIG. 3 (color online). Left: randomly generated points with $M_L \in [100, 1000]$ GeV, $M_E \in [100, 1000]$ GeV, $\bar{\lambda} < 0.5$, $\lambda = 0$, and $\lambda_{L,E}$ in the allowed ranges from precision EW data, plotted in the $\Delta a_\mu - m_\mu^{LE}/m_\mu$ plane. Both signs of couplings are allowed. The lightest mass eigenstate is required to satisfy the large electron positron limit. Different colors (shades) correspond to different regions of M_L in the order from top to bottom on the right side of the plot: $M_L < 150$ GeV, <250 GeV, <500 GeV, and <1000 GeV (the order is reversed on the left side of the plot). The horizontal line and dark (light) shaded bands correspond to the central experimental value of Δa_μ and 1σ (2σ) regions, respectively, specified in Eq. (28). Right: the same points as on the left plotted in the $\Delta a_\mu - R_{\mu\mu}$ plane.

expectation values replace the Higgs fields in the second term in Eq. (38). In the asymptotic case, $m_\mu^{LE}/m_\mu \simeq -1$, which also explains the anomaly, $R_{\mu\mu} \simeq 1$, which results from the first term in Eq. (38) being twice as large as in the SM and the same combinatoric factor of 3 with a minus sign from the second term.

From the qualitative discussion in the previous section, we expect that allowing nonzero λ should not change the results dramatically. This can be seen in Fig. 4, which is obtained under the same conditions as Fig. 3 with additional randomly generated $\lambda < 0.5$. An additional λ coupling has, however, important consequences for $h \to \gamma\gamma$. If both λ and $\bar{\lambda}$ are nonzero, the $h \to \gamma\gamma$ can be significantly modified. In Fig. 5, we plot the points from Fig. 4 in the $\Delta a_\mu - R_{\gamma\gamma}$ plane, where

$$R_{\gamma\gamma} = \frac{\Gamma(h \to \gamma\gamma)}{\Gamma(h \to \gamma\gamma)_{\rm SM}}. \tag{43}$$

In the plot on the left, the color notation is the same as in Fig. 4, namely, it represents different regions of M_L, while in the plot on the right, different colors (shades) represent the mass of the lightest mass eigenstate, which is more meaningful for $h \to \gamma\gamma$.

In the small M_L case, which can explain the muon $g-2$ within one standard deviation, the $R_{\gamma\gamma}$ can be decreased by about 25% or increased by about 15%. In the asymptotic case, $R_{\gamma\gamma}$ is negligibly modified in the region that explains the muon $g-2$ within one standard deviation.

Some of the results presented so far depend on our upper limit on possible Yukawa couplings, which we took to be 0.5. This upper limit is motivated by a simple UV embedding with nice features concerning the stability of the EW minimum of the Higgs potential, which we will discuss in the next section. This, however, is just one possibility, and in principle larger values of Yukawa couplings should be considered on phenomenological grounds. Thus, we also plot similar results assuming the upper limit for all Yukawa couplings to be 1.

The randomly generated points extended to $\bar{\lambda} < 1$ with $\lambda = 0$ are plotted in Fig. 6 in the $\Delta a_\mu - m_\mu^{LE}/m_\mu$ plane on the left and in the $\Delta a_\mu - R_{\mu\mu}$ plane on the right.

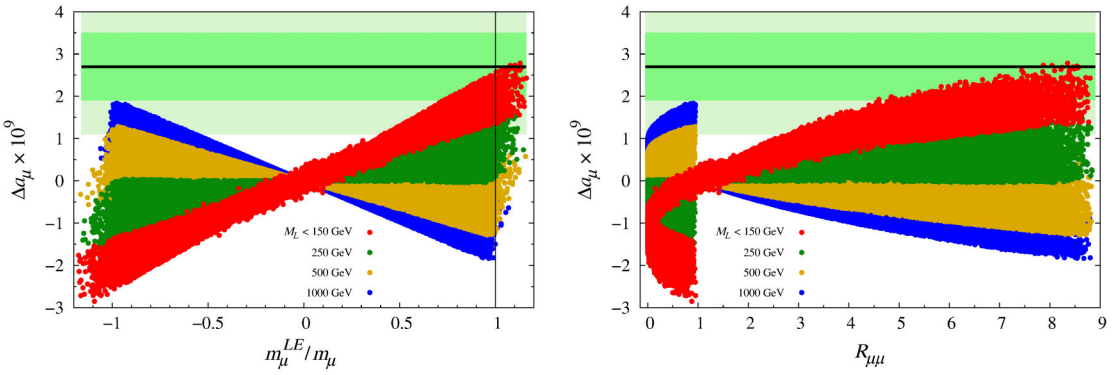

FIG. 4 (color online). The same as in Fig. 3 with additional randomly generated $\lambda < 0.5$.

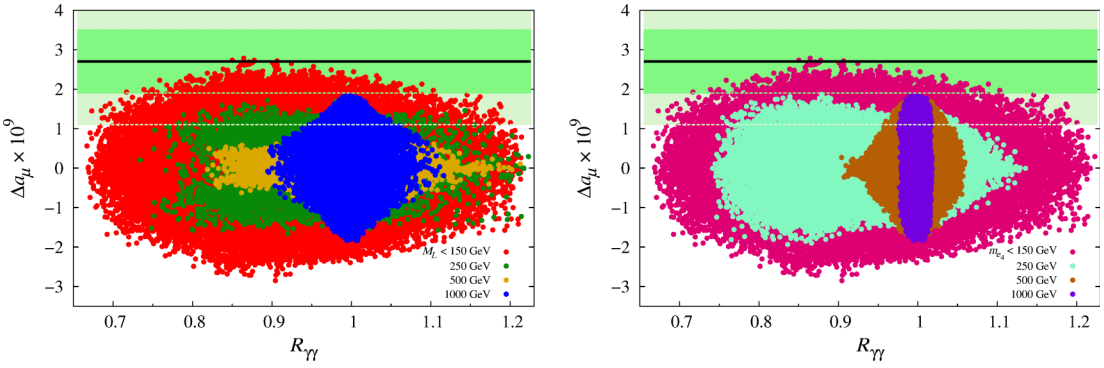

FIG. 5 (color online). Left: the same as in Fig. 4 plotted in the $\Delta a_\mu - R_{\gamma\gamma}$ plane. Right: the same as on the left, but different colors (shades) represent the mass of the lighter extra charged lepton mass eigenstate, m_{e_4}, in ranges <150 GeV, <250 GeV, <500 GeV, and <1000 GeV when going from outside toward the center.

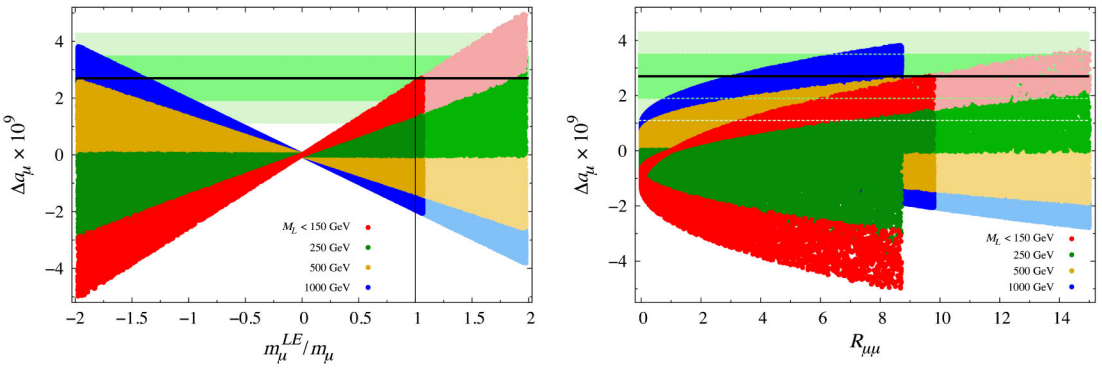

FIG. 6 (color online). The same as in Fig. 3 with the region of $\bar{\lambda}$ extended to $\bar{\lambda} < 1$. The lightly shaded points are excluded by the ATLAS search for $h \to \mu^+\mu^-$. The plot on the right would extend to larger values of $R_{\mu\mu} \simeq 24$.

Comparing Figs. 3 and 6 clearly demonstrates the effect of varying $\bar{\lambda}$ coupling; increasing $\bar{\lambda}$ extends the plots to larger values of both Δa_μ and m_μ^{LE}/m_μ, while the correlation of these contributions is unchanged. The Higgs coupling to the muon is modified more dramatically, and part of the parameters space is already ruled out by the ATLAS search for $h \to \mu^+\mu^-$ [6] (lightly shaded regions in both plots). The $R_{\mu\mu}$ ranges between 6 and 9.8 (the current limit) in the small M_L case that can explain the muon $g-2$ anomaly and between 1 and 9 in the asymptotic case.

The addition of $\lambda < 1$ somewhat expands the ranges of Δa_μ, m_μ^{LE}/m_μ, and $R_{\mu\mu}$ for all regions of M_L, which can be seen in Fig. 7. Nevertheless, as expected, the plots in Figs. 6 and 7 look qualitatively very similar.

Increasing $\bar{\lambda}$ and λ up to 1 significantly extends ranges of predictions for $R_{\gamma\gamma}$, given in Fig. 8, especially for the asymptotic case. In the small M_L case that can explain the

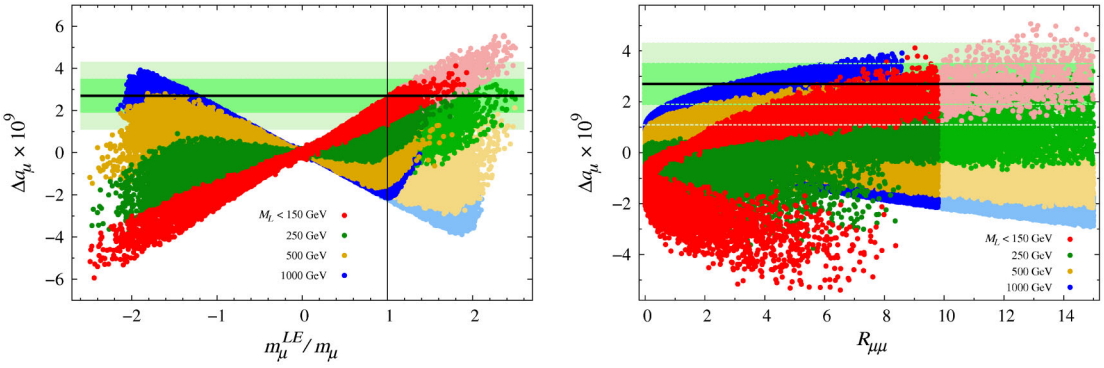

FIG. 7 (color online). The same as in Fig. 6 with additional randomly generated $\lambda < 1$.

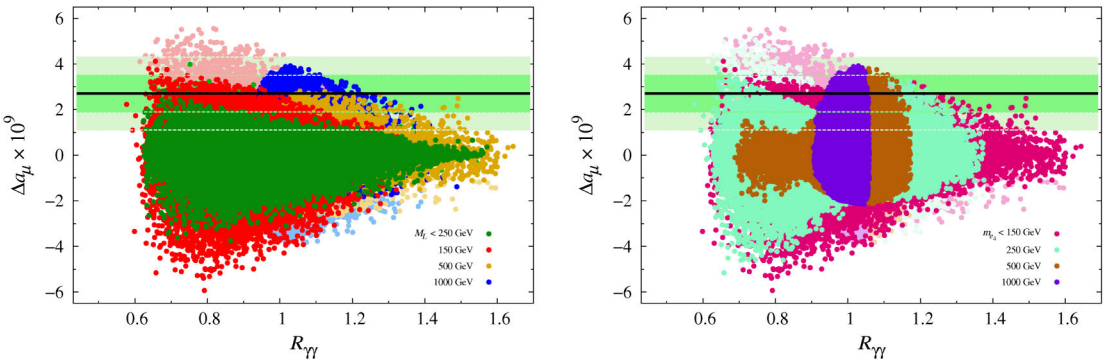

FIG. 8 (color online). Left: the same as in Fig. 4 plotted in the $\Delta a_\mu - R_{\gamma\gamma}$ plane. Right: the same as on the left, but different colors (shades) represent the mass of the lighter extra charged lepton mass eigenstate, m_{e_4}, in ranges <150 GeV, <250 GeV, <500 GeV, and <1000 GeV when going from the outside toward the center. The lightly shaded points are excluded by the ATLAS search for $h \to \mu^+\mu^-$.

muon $g-2$ anomaly within 1σ, the $R_{\gamma\gamma}$ ranges between 0.6 and 1.15; while in the asymptotic case, the $R_{\gamma\gamma}$ ranges between 0.9 and 1.5. In addition, the range of possible masses of the lightest extra charged lepton significantly expands; see Fig. 8 on the right. With $\bar{\lambda}$, $\lambda < 1$ for the small M_L case that can explain the muon $g-2$ anomaly within 1σ, the mass of the lightest extra charged lepton, m_{e_4}, has to be at most $\sim$250 GeV, while with $\bar{\lambda}$, $\lambda < 0.5$, the maximum mass is only $\sim$150 GeV.

D. Light charged leptons at the LHC

This scenario, especially the small M_L case that can explain the muon $g-2$ anomaly, could be searched for at the LHC. The LHC phenomenology of extra leptons was discussed, for example, in Refs. [3,5,25,26]. The pair production cross section of extra leptons with masses of order 100 GeV is about 1 pb at the LHC at 8 TeV (and it is steeply falling with increasing the mass). Extra leptons decay into Z, W, or h and a light lepton. The decay branching ratios are typically comparable, and so the signatures of this scenario are spread over a variety of final states. Especially for small masses of charged leptons, the branching ratios highly depend on the Yukawa couplings.

So far, limited searches have been done. A search motivated by heavy leptons specific to type III seesaw models limits $\sigma(pp \to L^0 L^\pm) \times B(L^\pm \to Z l^\pm) \times B(L^0 \to W l)$, where l is either e or μ, to about 200 fb for heavy leptons with the mass 100 GeV [27]. There is also a similar search at CMS for both heavy leptons decaying through W [28]. In addition to these specific searches, there are also general searches for the anomalous production of multilepton events [29] that constrain specific decay modes of heavy leptons.

However, in addition to the dependance of the branching ratios on Yukawa couplings within the scenario we discussed, these in principle also depend on couplings that are not necessary for the explanation of the muon $g-2$. For example, heavy leptons can dominantly decay into τ leptons, reducing the number of light leptons in final states. Due to limited existing constraints, all the scenarios we discuss are or easily can be made viable. This could dramatically change with further searches for heavy leptons covering all the decay modes in near future. In addition, improving the limits on $h \to \mu^+\mu^-$, which already constrain parts of the parameter space, is highly motivated even if the sensitivity to the SM prediction for this process cannot be reached soon.

Finally, the charged leptons relevant to the asymptotic solution are far beyond the current reach of the LHC. However, this solution can still be highly constrained by improving the limits on $h \to \mu^+\mu^-$.

IV. POSSIBLE UV COMPLETION

The model with extra vectorlike leptons can be embedded into recently discussed scenario with extra three or more complete vectorlike families [13,14]. This scenario features gauge coupling unification, a sufficiently stable proton, and the Higgs quartic coupling remaining positive all the way to the GUT scale. Predicted values of gauge couplings at the electroweak scale are highly insensitive to GUT scale parameters and masses of vectorlike fermions. They can be understood from IR fixed point predictions and threshold effects from integrating out vectorlike families.

These features are preserved even when one generation of L and E has masses close to the EW scale and the extra Yukawa couplings are of the size required to obtain the measured value of the muon magnetic moment. A specific example assuming extra three complete vectorlike familes is given in Fig. 9. We fix M_{L_1} and M_{E_1} to 150 GeV (even sizable variations of these masses would have a negligible impact on the results presented in this section) and $\bar{\lambda}$ to 0.5. This value of $\bar{\lambda}$ and the masses of vectorlike leptons can generate muon $g-2$ close to the central value and simultaneously generate the muon mass completely from the mixing between light and heavy families. The masses of the other two generations of vectorlike leptons and all three

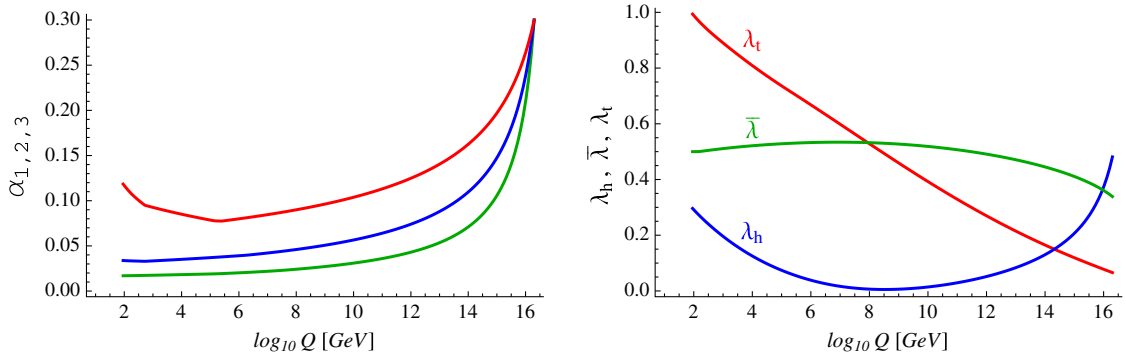

FIG. 9 (color online). Left: the RG evolution of gauge couplings, α_3 (top), α_2 (middle), and α_1 (bottom), in the SM extended by three vectorlike families for $\alpha_G = 0.3$ at $M_G = 2 \times 10^{16}$ GeV. Right: the RG evolution of the Higgs quartic coupling for $m_h = 126$ GeV, the top Yukawa coupling, and the $\bar{\lambda}$ with the EW scale value of 0.5. The masses of vectorlike fermions are $M_{L_1} = M_{E_1} = 150$ GeV, $M_{L_{2,3}} = 2.0 \times 10^6$ GeV, $M_{E_{2,3}} = 2.4 \times 10^7$ GeV, $M_Q = 520$ GeV, $M_U = 1.4 \times 10^5$ GeV, and $M_D = 2.5 \times 10^5$ GeV.

generations of quarks are varied to obtain the measured values of gauge couplings at the EW scale starting from $\alpha_G = 0.3$ at $M_G = 2 \times 10^{16}$ GeV. We set all other Yukawa couplings to zero, except for the top quark Yukawa. The contributions from λ^L and λ^E to the renormalization group (RG) evolution of gauge, top Yukawa, and Higgs quartic couplings can also be neglected when the constraints from precision EW data are satisfied. The analysis closely follows Refs. [13,14] with the only exception that we use 1-loop RG equations for Yukawa and Higgs quartic couplings. We use 2-loop RG equations for gauge couplings as in Refs. [13,14].

The evolution of gauge couplings is almost identical to examples given in Refs. [13,14]. With zero Yukawa couplings of vectorlike fermions, the evolution of gauge couplings only depends on the geometric means of masses of vectorlike fermions with the same quantum numbers. Fixing two masses, M_{L_1} and M_{E_1}, to 150 GeV is compensated by making masses of the other two vectrolike families correspondingly heavier. The addition of $\bar{\lambda} = 0.5$ does not change the evolution of gauge couplings much since Yukawa couplings contribute only at the 2-loop level.

The evolution of Higgs quartic coupling depends significantly on Yukawa couplings present in the model. In the standard model, the top Yukawa coupling already drives Higgs quartic coupling to negative values at a high scale. Additional sizable Yukawa couplings accelerate this behavior, and thus the stability of the EW minimum sets a limit on the size of extra Yukawa couplings.

In the case of the SM extended by three vectorlike families, the RG evolution of Higgs quartic coupling is significantly different. The Higgs quartic coupling can remain positive all the way to the GUT scale even with additional Yukawa couplings. The difference comes from larger values of all gauge couplings compared to the SM above the scale of vectorlike fermions. Larger gauge couplings slow down the running of Higgs quartic coupling, see Fig. 9, and eventually turn the beta function of Higgs quartic coupling positive. This effect is further amplified by the fact that the top Yukawa is driven fast to much smaller values compared to the SM (again due to larger gauge couplings), and its contribution to the running of Higgs quartic coupling becomes small.

This is the minimal scenario (in this framework) with gauge coupling unification, sufficiently stable proton, and the Higgs quartic coupling remaining positive all the way to the GUT scale that simultaneously explains the deviation in the muon magnetic moment and generates the correct muon mass. Adding another lepton Yukawa coupling of the same size, for example λ to also modify $h \to \gamma\gamma$, would make the Higgs quartic coupling briefly go negative. The EW minimum would still be sufficiently long lived even with somewhat larger values of lepton Yukawa couplings. Alternatively, a stable EW minimum can be obtained (the Higgs quartic coupling is positive all the way to the GUT scale) by lowering both extra lepton Yukawas to ~ 0.4.

V. CONCLUSIONS

We showed that the deviation of the measured value of the muon anomalous magnetic moment from the standard model prediction can be completely explained by mixing of the muon with extra vectorlike leptons, L and E, near the electroweak scale. This mixing simultaneously contributes to the muon mass (we label this contribution by m_μ^{LE}), and the correlation between contributions to the muon mass and muon $g-2$ is controlled by the mass of the neutrino originating from the doublet L, which is given by the vectorlike mass parameter M_L.

We have found two generic solutions: the asymptotic one, $M_L \gg M_Z$, in which case the Higgs loop dominates and the measured value of the muon $g-2$ is obtained for $m_\mu^{LE}/m_\mu \simeq -1$, and the second one with a light extra neutrino, $M_L \simeq M_W$, in which case the W loop dominates and the measured value of the muon $g-2$ is obtain for $m_\mu^{LE}/m_\mu \simeq +1$. In the first case, about twice as large a contribution from the direct Yukawa coupling of the muon is required to generate the correct muon mass, while in the

second case, the muon mass can fully originate from the mixing with heavy leptons.

The sizes of possible contributions to the muon $g-2$, muon mass, and other observables depend on the upper limit on Yukawa couplings that we allow in the model. We considered two cases, the upper limit being 0.5 and 1. The 0.5 upper limit is motivated by a simple UV embedding of this scenario with three complete vectorlike families featuring gauge coupling unification, a sufficiently stable proton, and the Higgs quartic coupling remaining positive all the way to the GUT scale.

With the upper limit on Yukawa couplings being 0.5, the muon $g-2$ can be explained within one standard deviation either with $M_L \lesssim 130$ GeV (the mass of the lightest extra charged lepton is $m_{e_4} \lesssim 150$ GeV) or with $M_L \gtrsim 1$ TeV. The small M_L case predicts the $h \to \mu^+\mu^-$ in the range 5–9 times the standard model prediction. Depending on additional Yukawa coupling, the branching ratio for $h \to \gamma\gamma$ can be enhanced by $\sim 15\%$ or lowered by $\sim 25\%$ from its SM prediction. The asymptotic case predicts only very small modifications of $h \to \mu^+\mu^-$ and $h \to \gamma\gamma$ compared to the SM.

Allowing Yukawa couplings of order 1, the range of parameters that can explain the muon $g-2$ within one standard deviation and the range of predictions for Higgs branching ratios significantly expand. The small M_L case now requires $M_L \lesssim 200$ GeV (the mass of the lightest extra charged lepton is $m_{e_4} \lesssim 250$ GeV). The predicted $h \to \mu^+\mu^-$ ranges from 0.5 to 24 times the standard model prediction. A part of the parameter space is thus already excluded by the ATLAS search for this decay mode of the Higgs (the upper limit is 9.8 times the SM prediction). Depending on additional Yukawa coupling, the $h \to \gamma\gamma$ rate can be modified by $\sim 50\%$.

New vectorlike leptons generically predict a variety of flavor violating processes. The existing limits set strong constraints on other possible couplings in the model besides those needed for the explanation of the muon $g-2$ anomaly. In addition, extra charged leptons provide a variety of signatures at the LHC. They can be pair produced or can modify Higgs decays. Some searches are already excluding parts of the parameter space, and others are getting close. Covering all possible decay modes of extra leptons should allow us to fully explore the small M_L case at the LHC with already available data.

ACKNOWLEDGMENTS

R. D. thanks H. D. Kim for useful discussions. A. R. thanks K. Kannike for comparing the results of calculations. R. D. also thanks Seoul National University and the KITP UCSB for kind hospitality during final stages of this project. This work was supported in part by the Department of Energy under Grant No. DE-FG02-91ER40661.

[1] For a review and references, see, for example, F. Jegerlehner and A. Nyffeler, Phys. Rep. **477**, 1 (2009).
[2] A. Czarnecki and W. J. Marciano, Phys. Rev. D **64**, 013014 (2001).
[3] K. Kannike, M. Raidal, D. M. Straub, and A. Strumia, J. High Energy Phys. 02 (2012) 106; 10 (2012) 136(E).
[4] B. Murakami, Phys. Rev. D **65**, 055003 (2002).
[5] G. F. Giudice and O. Lebedev, Phys. Lett. B **665**, 79 (2008).
[6] ATLAS Collaboration, Report No. ATLAS-CONF-2013-010.
[7] A. Joglekar, P. Schwaller, and C. E. M. Wagner, J. High Energy Phys. 12 (2012) 064.
[8] N. Arkani-Hamed, K. Blum, R. T. D'Agnolo, and J. Fan, J. High Energy Phys. 01 (2013) 149.
[9] L. G. Almeida, E. Bertuzzo, P. A. N. Machado, and R. Z. Funchal, J. High Energy Phys. 11 (2012) 085.
[10] J. Kearney, A. Pierce, and N. Weiner, Phys. Rev. D **86**, 113005 (2012).
[11] ATLAS Collaboration, Report No. ATLAS-CONF-2013-012.
[12] CMS Collaboration, Report No. CMS-PAS-HIG-13-001.
[13] R. Dermisek, Phys. Lett. B **713**, 469 (2012).
[14] R. Dermisek, Phys. Rev. D **87**, 055008 (2013).
[15] R. Dermisek, S.-G. Kim, and A. Raval, Phys. Rev. D **84**, 035006 (2011).
[16] R. Dermisek, S.-G. Kim, and A. Raval, Phys. Rev. D **85**, 075022 (2012).
[17] G. W. Bennett *et al.* (Muon $g-2$ Collaboration), Phys. Rev. D **73**, 072003 (2006).
[18] T. Aoyama, M. Hayakawa, T. Kinoshita, and M. Nio, Phys. Rev. Lett. **109**, 111808 (2012).
[19] K. Hagiwara, R. Liao, A. D. Martin, D. Nomura, and T. Teubner, J. Phys. G **38**, 085003 (2011).
[20] M. Davier, A. Hoecker, B. Malaescu, and Z. Zhang, Eur. Phys. J. C **71**, 1515 (2011); **72**, 1874(E) (2012).
[21] J. P. Leveille, Nucl. Phys. **B137**, 63 (1978).
[22] K. R. Lynch, arXiv:hep-ph/0108081.
[23] J. Beringer *et al.* (Particle Data Group), Phys. Rev. D **86**, 010001 (2012).
[24] K. Kannike (private communication).
[25] E. Del Nobile, R. Franceschini, D. Pappadopulo, and A. Strumia, Nucl. Phys. **B826**, 217 (2010).
[26] S. P. Martin, Phys. Rev. D **81**, 035004 (2010).
[27] ATLAS Collaboration, Report No. ATLAS-CONF-2013-019.
[28] S. Chatrchyan *et al.* (CMS Collaboration), Phys. Lett. B **718**, 348 (2012).
[29] S. Chatrchyan *et al.* (CMS Collaboration), J. High Energy Phys. 06 (2012) 169.